

METABOLITES PROFILE OF COLORECTAL CANCER CELLS AT DIFFERENT STAGES

HAZWANI MOHD YUSOF¹, SHARANIZA AB-RAHIM¹, WAN ZURINAH WAN NGAH², SHEILA NATHAN³,
RAHMAN A. JAMAL A.⁴, MUSALMAH MAZLAN^{1*}

¹Department of Biochemistry and Molecular Medicine, Faculty of Medicine, Universiti Teknologi MARA, Campus Sungai Buloh, 47000 Sungai Buloh, Selangor, Malaysia. ²Universiti Kebangsaan Malaysia Medical Centre, Jalan Yaacob Latif, Bandar Tun Razak, 56000 Batu 9 Cheras, Wilayah Persekutuan Kuala Lumpur, Malaysia. ³Department of Biosciences and Biotechnology, Faculty of Science and Technology, Universiti Kebangsaan Malaysia, 43600 UKM Bangi, Selangor, Malaysia. ⁴UKM Medical Molecular Biology Institute, UKM Medical Centre, Jalan Yaacob Latif, Bandar Tun Razak, 56000 Cheras, Kuala Lumpur, Malaysia. Email: musalmah6393@salam.uitm.edu.my

Received: 24 January 2019, Revised and Accepted: 25 July 2019

ABSTRACT

Objective: The aim of this study is to characterize the metabolite profiles of colorectal cancer (CRC) cells of different stages of the disease to understand the pathophysiological changes that may help to identify prevention strategies as well as the sites for potential therapeutic drug actions.

Methods: Six CRC cell lines of different stages (classified using the Dukes classification) were used, and they are SW 1116 (stage A), HT 29 and SW 480 (stage B), HCT 15 and DLD-1 (stage C), and HCT 116 (stage D). Metabolites were extracted using methanol and water, and metabolic profiling was performed using liquid chromatography-mass spectrometry. Mass profiler professional software was used for statistical analysis.

Results: There were 111,096 compounds detected across the samples, and 24 metabolites were identified to be significantly different between the CRC stages. Most notably, there were eight metabolites that were significantly upregulated in the more advanced stages (B, C, and D) compared with Stage A. These metabolites include flavin mononucleotide, l-methionine, muricatacin, amillaripin, 2-methylbutyrylcarnitine, lumichrome, hexadecanoic acid, and lysoPE (0:0/16:0).

Conclusion: This study showed that the expressions of metabolites at different stages of CRC were different, which represent the metabolic changes occurring as CRC advances. The knowledge may help identify biomarkers for the staging of CRC, which could improve its prognosis as well as provide a basis for the development of therapeutic interventions.

Keywords: Colorectal cancer, Metabolomics, Cancer stages.

© 2019 The Authors. Published by Innovare Academic Sciences Pvt Ltd. This is an open access article under the CC BY license (<http://creativecommons.org/licenses/by/4.0/>) DOI: <http://dx.doi.org/10.22159/ijap.2019.v11s1.T0051>

INTRODUCTION

Colorectal cancer (CRC) is the third most commonly diagnosed cancer and the second most deadly [1]. Its incidence is higher in more developed countries although the trend is increasing in developing countries [2].

CRC is classified using various types of classifications. Dukes' classification is widely used and is the predecessor of the current tumor node metastasis staging system [3]. The current gold standard for CRC diagnosis and staging is based on colonoscopy combined with histopathological examination [4]. However, these tools are invasive and sometimes do not accurately identify the stages of CRC [5]. Early diagnosis is important as the 5-year survival rate, in advanced CRC is lower than 10%, whereas treatment instituted at an earlier stage has a survival rate of up to 90% [6]. In addition, accurate staging is also necessary as treatment strategies for CRC are based on the stage of the disease [7]. Therefore, there is a need for non-invasive methods for early diagnosis and staging for improvement in the prognosis of the disease.

Until today, different new treatment strategies for CRC are still being investigated with the aims to preserve patients' quality of life. However, developments of new treatment strategies are hampered by a lack of understanding of pathogenesis and pathophysiology of the disease progression.

Metabolomics interprets the metabolic profile in a complex system using the combination of data from analytical techniques (nuclear magnetic resonance and mass spectrometry) and multivariate data analysis [8]. This approach has been used in several fields including oncology. CRC

metabolomics studies have been widely conducted on human biological samples [9-11]. There were also several metabolomics studies conducted comparing the metabolite profiles at different stages of CRC using human tissue samples [12-15] with successful results on biomarkers discovery for early CRC detection and prognosis. However, the metabolic changes identified among the populations were diverse and difficult to conclude [16]. Despite this information, the metabolic changes leading to increase the severity of this disease, especially at the molecular level, are still unclear.

Studies of metabolic profiles in cell culture are highly valuable [17] as they are able to provide important information regarding the molecular mechanism of disease progression. *In vitro* studies have been used to develop models of biological pathways and networks affected in disease [18,19].

In this study, we aim to identify the metabolic changes that occur in CRC cells at different stages of the disease. Non-targeted metabolomics was used to characterize the intracellular metabolic profiles of CRC cells of different stages. Identification of the cellular metabolite profiles of the different cell lines may lead to the possibility of using cell culture in place of animal models in CRC study, especially in testing treatment modality. Our analysis revealed that there were differences in the metabolic profiles in CRC cells at different stages.

METHODS

Cell culture

Established CRC cell lines classified using the Dukes classification were used. These include SW 1116 (Stage A), HT 29 and SW 480 (Stages B),

HCT 15 and DLD-1 (Stage C), and HCT 116 (Stage D) (AddexBio, USA). CRC cells were grown in DMEM high glucose medium (Gibco, Invitrogen, USA) supplemented with 10% fetal bovine serum (Gibco, Invitrogen, USA) and 1% penicillin-streptomycin (Gibco, Invitrogen, USA) and incubated at 37°C with 98% humidity of 5% (v/v) CO₂ incubator (Binder, Germany).

Preparation of intracellular metabolite extract

Preparation of intracellular metabolite extract was performed according to a previous study [20]. CRC cells were seeded in 6 well plates, 1×10⁶ cells per well and incubated overnight in an incubator. Once the cells have attached to the surface of the well plate, the plate was placed on wet ice to slow down metabolism. Media was removed and cells were washed 3 times with ice-cold phosphate buffer saline (Gibco, Invitrogen, USA). Subsequently, 1 ml of extraction solvent methanol-water (8:2, v/v), pre-cooled in -80°C for at least 1 h, was added to each well plate containing cells and then placed at -80°C for 15 min. Cells were scraped and the suspension was transferred into a microcentrifuge tube. The suspension was then centrifuged at 16,000 rpm for 10 min at 4°C (Eppendorf 5424 R, USA). The supernatant was transferred into a new microcentrifuge tube, and the extract was dried in a concentrator (Eppendorf, USA). The dry samples were stored at -80°C until analysis. Every extraction sample was prepared in three biological replicates.

Liquid chromatography-mass spectrometry (LC-MS) Q-TOF analysis for metabolomics

Dried samples were dissolved with 30 µl mobile phase acetonitrile-water (1:1, v/v) and vortex for 1 min. Samples were centrifuged at 10,000 rpm, 4°C for 10 min. Samples analysis was performed on LC-MS Q-TOF (Agilent Technologies 6520, USA) system. The analysis was performed in three technical replicates and three biological replicates with positive and negative modes. The acquired LC-MS Agilent 6520 Q-TOF mass spectrometer data were processed as described in a previous study [21]. LC-MS Q-TOF equipment with an ESI source was used to analyze the samples together with a 1200 rapid resolution system (Agilent Technologies, USA). For chromatographic separation, column ZORBAX Eclipse Plus C18 600 Bar, 2.1×100 mm, 1.8 µm particle size (Agilent Technologies, USA) was used, and during analysis, the temperature was maintained at 40°C. The injection volume was 2 µl with a flow rate of 0.25 ml/min. Development of a linear gradient was performed over 36 min from 5% to 95% of the mobile phase (0.1% formic acid in ACN). Each analysis used 48 min run times. Setting for ESI source was V Cap 4000 V, skimmer 65 V, and fragmentor 125 V. The nebulizer was set at 45 psig and the nitrogen drying gas was set at a flow rate of 12 l/min. Drying gas temperature was maintained at 350°C. Data were acquired at a rate of 2.5 spectra/s with a stored mass range of m/z 50–1000. Auto calibration was performed before each batch of analysis and reference mass correction was enabled throughout the run. The mass spectrometer was tuned to allow detection of compounds at accuracy of ±2 ppm before the analysis. To track the uniformity of each extraction, an extracted pool samples were run during along with the samples and were served as a quality control.

Data processing

Agilent MassHunter Workstation Data Acquisition software and Agilent MassHunter Qualitative Analysis software (Agilent Technologies, USA) were used for data collection and data processing, respectively. Step for data processing included molecular feature extraction, background subtraction, data filtering, statistical analysis by ANOVA, and principal component analysis (PCA), followed by database search and alignment. For each sample, the compound exchange format file was created and further analyzed using mass profile professional (MPP) (Agilent Technologies, USA). Endogenous and exogenous metabolites were identified using metabolite identification software, METLIN Personal Metabolite Database, and MPP (Agilent Technologies, USA).

Data analysis

Molecular Feature Extractor (MFE) algorithm in the MassHunter workstation software was used for data mining. Absolute height

parameter was set at 200, and all entities presented with less than this abundance level were considered as noise and removed. Setting for data processing method was used to process all generated data files in a batch mode. The first filter (frequency analysis) determined the compounds (entities) that were present 100% of the time in at least one studied group. The second filter of frequency selected entities that were present in at least 100% of samples. Analysis of variance (ANOVA) was the next step for filtering in selecting entities that were significantly different between the four experimental groups. Next, fold change of two and above was set for identification of metabolites with differential differences in abundance between the experimental groups and was also used to eliminate possible discriminating compounds. Data recursion was then performed, which re-examined data to ensure that each entity is real. Automatically, the software re-extracted the final group of metabolites from the data to generate extracted ion chromatograms (EICs). The peak inspection of resulted EICs was conducted to eliminate the false positives and false negatives. Finally, the confirmed metabolites were statistically analyzed.

Statistical analysis and visualization

MPP software (Agilent Technologies, USA) was used for statistical analysis and visualization of metabolite profiles. Analysis of one-way ANOVA with Benjamini-Hochberg multiple testing correction was used to determine significant differences in the abundance of the compound between four different groups. Metabolomics pathway analysis (Metaboanalyst 3.5) software was used to determine partial least squares-discriminant analysis (PLS-DA) score plot, PCA score plot, and variable importance in projection (VIP). VIP score close to or greater than one can be considered important in a given model.

RESULTS AND DISCUSSION

In this study, the CRC cell lines were classified into the various stages according to Dukas classification as described by ATCC and a previous study [22,23]. A total of six CRC cell lines were analyzed. LC/MS analysis detected 68,197 (positive mode), and 42,899 (negative mode) compounds across the entire range of samples. Fig. 1 shows the workflow analysis process using MPP software. Using these criteria, 24 known metabolites were identified to be significantly altered between the stages.

Table 1 shows the significant differences and the fold change of metabolites expressed by CRC cells at Stages B, C, and D compared to Stage A. Fold change with a positive value indicates a relatively higher level of metabolites while a negative value indicates a relatively lower level compared to Stage A. The data showed that eight metabolites were significantly upregulated in all three stages (B-D). These were flavin mononucleotide (FMN), l-methionine, muricatacin, amillaripin, 2-methylbutyrylcarnitine, lumichrome, hexadecanoic acid, and lysoPE (0:0/16:0). The level of pipericine, acetylcarnitine, and glucose 6-phosphate was found to be lower in Stage B but was significantly increased in Stages C and D. The level of flavin adenine dinucleotide (FAD)

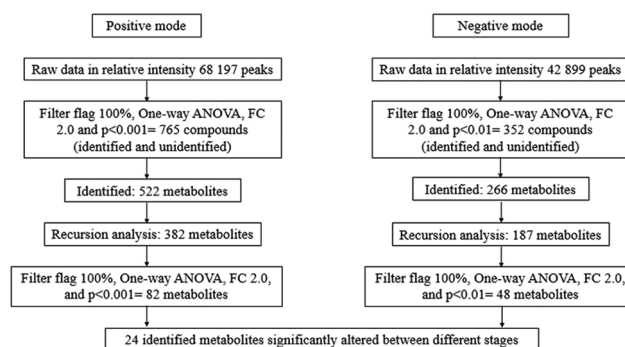


Fig. 1: Workflow analysis process using mass profile professional software

Table 1: Metabolites found to be differentially abundant between colorectal cancer cell lines of Stage A and Stages B, C, and D

Metabolites	Log fold change relative to Dukes' A			p
	B versus A	C versus A	D versus A	
FAD	-14.84	-14.59	2.65	5.95×10 ⁻³¹
G6P	-0.04	0.62	15.16	4.17×10 ⁻³⁰
L-Phenylalanine	21.61	20.99	-0.91	2.19×10 ⁻²⁹
LysoPE (22:6 (4Z, 7Z, 10Z, 13Z, 16Z, 19Z)/0:0)	14.50	15.47	-0.91	7.81×10 ⁻²⁸
Armillaripin	5.11	5.05	4.86	1.29×10 ⁻²⁵
Phytosphingosine	1.06	-13.05	1.08	5.08×10 ⁻²⁴
LysoPE (0.0/16:0)	0.62	1.47	2.57	2.77×10 ⁻¹⁸
Pantothenic acid	21.57	16.22	-0.91	1.61×10 ⁻¹⁷
Riboflavin	-0.94	-2.24	-2.13	5.26×10 ⁻¹⁶
LysoPE (0:0/16:1 (9Z))	9.28	15.94	-0.91	1.03×10 ⁻¹⁵
LysoPE (0:0/20:4 (5Z, 8Z, 11Z, 14Z))	-0.72	-1.92	-1.06	1.16×10 ⁻¹⁴
L-Methionine	1.14	12.07	16.46	6.32×10 ⁻¹²
Acetylcarnitine	-0.76	2.00	2.71	1.77×10 ⁻¹²
FMN	12.37	13.78	15.63	3.46×10 ⁻¹¹
1,2,4-Nonadecanetriol	3.57	-12.36	0.34	2.74×10 ⁻¹¹
Muricatacin	11.51	11.48	9.39	1.83×10 ⁻¹⁰
L-Lactic acid	-14.08	-14.26	2.42	2.04×10 ⁻⁹
(Z)-13-Oxo-9-octadecenoic acid	-6.56	-12.61	-0.33	1.48×10 ⁻⁸
2-Methylbutyrylcarnitine	1.55	0.42	0.19	6.90×10 ⁻⁶
Lumichrome	7.76	6.40	8.17	8.87×10 ⁻⁵
Hexadecanoic acid	5.99	5.92	5.64	2.04×10 ⁻⁵
Pipericine	-6.90	0.38	5.30	4.77×10 ⁻⁴
LysoPE (20:5 (5Z, 8Z, 11Z, 14Z, 17Z)/0:0)	-1.26	-4.20	-1.85	3.24×10 ⁻⁴
L-Leucine	-4.24	-11.23	-2.81	6.69×10 ⁻³

FAD: Flavin adenine dinucleotide, FMN: Flavin mononucleotide, G6P: Glucose 6-phosphate

and l-lactic acid was significantly lower in Stages B, C, and D. The levels of (Z)-13-Oxo-9-octadecenoic acid, lysoPE(0:0/20:4(5Z,8Z,11Z,14Z)), lysoPE(20:5(5Z,8Z,11Z,14Z,17Z)/0:0), riboflavin, and l-leucine were lower in all three stages compared with A. Moreover, the levels of pantothenic acid, l-phenylalanine, lysoPE(22:6(4Z,7Z,10Z,13Z,16Z,19Z)/0:0), and lysoPE(0:0/16:1(9Z)) were significantly increased in Stages B and C but were lower in D.

PLS-DA analysis (Fig. 2) showed differences in the metabolite expression signatures clusters between the different stages. Results showed separation between all CRC stages. When the PCA was used to compare the metabolic patterns between two different groups, the results showed that there were significant changes between the cells of different stages (Fig. 3).

Fig. 4 showed that l-methionine, FMN, and glucose 6-phosphate (G6P) were the top three most important metabolites affected in CRC based on the VIP score. L-methionine is an essential amino acid and plays important role in metabolism [24]. The result showed that l-methionine was significantly increased in the more advanced stages. In every cell, methionine is partitioned between protein synthesis and the *de novo* pathway. Cancer cells are dependent on methionine [25,26]. This phenomenon is probably due to one or a combination of deletions, polymorphisms, or alterations in the expression of genes in the methionine *de novo* and salvage pathway [26]. There are *in vitro* and *in vivo* studies which showed that methionine-restricted diet inhibits cancer growth and prolonged a healthy life-span [27] suggesting that cancer cells require high levels of methionine compared to normal cells.

Riboflavin, FMN, and FAD are involved in riboflavin metabolism. The present finding showed that riboflavin was downregulated while FMN and FAD were upregulated as the stages of CRC advances. Riboflavin metabolism is associated with ATP production, ROS production, antioxidant defense, DNA repair, protein folding, apoptosis, and chromatin remodeling [28]. Low intake of riboflavin affects the levels of FMN and FAD in cells. Low riboflavin status is associated with increased homocysteine concentration, which probably results in lower availability of methyl groups [29]. In fact, low intake of dietary riboflavin was reported to be associated with colorectal adenomas [30]. Depletion

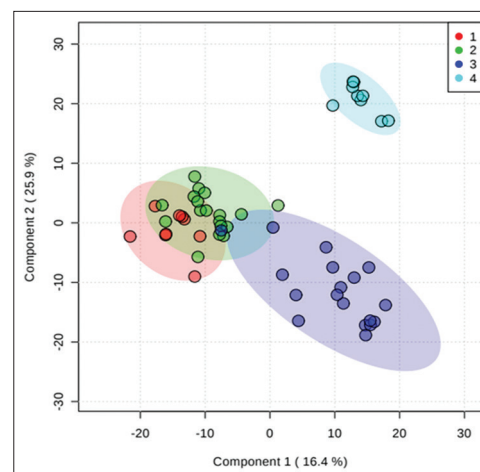


Fig. 2: Partial least squares-discriminant analysis scores plot discriminating colorectal cancer (CRC) cell lines from different stages. The numbers represent the stage of CRC as follows: 1= Stage A, 2= Stage B, 3= Stage C, 4= Stage D

of riboflavin in cells also led to enhanced production of reactive oxygen species and affected cell cycle progression and cell growth [31].

In the present study, G6P was significantly altered; its level was lower in Stage B but increased at the later Stages (C and D). G6P is a product from the conversion of glucose that involved in glycolysis and pentose phosphate pathway [32]. Changes of G6P level could indicate one of the mechanisms of cancer cells in regulating the Crabtree effect [33]. The tumor cell lines with high glycolytic rates also exhibit the Crabtree effect [34].

The present findings also revealed that several lipids were downregulated in the later stages. (Z)-13-Oxo-9-octadecenoic acid and lysoPE(0:0/20:4(5Z,8Z,11Z,14Z)), lysoPE(20:5(5Z,8Z,11Z,14Z,17Z)/0:0) were the metabolites affected. This finding is in agreement with a previous CRC metabolomics study

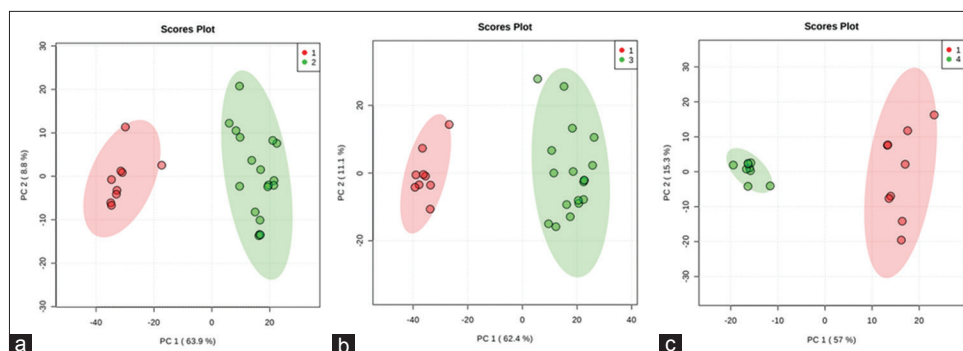


Fig. 3: (a-c) Principal component analysis score plots based on various stages of colorectal cancer cells compared to Stage A. The numbers in the graphs represent the stages where 1 = Stage A, 2 = Stage B, 3 = Stage C and 4 = Stage D. Plot I; Stage B versus A, Plot II; Stage C versus A, Plot III; Stage D versus A

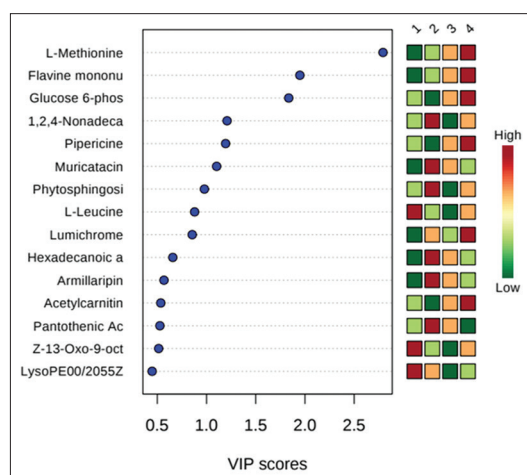


Fig. 4: Variable importance in projection scores identified by partial least squares-discriminant analysis

that used tissues from CRC patients [13]. Lipids are a diverse group of metabolites and they have several key biological functions, such as structural components of cell membranes, energy storage sources, and intermediates in signaling [35]. Alteration of lipid metabolism is an established hallmark of cancer. In cancer, all of these processes are critical for generating the membrane constituents, energetic, biophysical, and signaling pathways that drive diverse aspects of tumorigenesis [36].

CONCLUSIONS

To the best of our knowledge, this is the first study to characterize the metabolic profiles of CRC cell lines at varying stages of the disease. This study highlights the metabolites changes in CRC cells at different stages. The characterization is important in the development of *in vitro* models for drug testing and to understand the pathogenesis during the CRC progression.

ACKNOWLEDGMENT

This study was supported by Long Term Research Grant, No: LRGS/2014/ UKM-UiTM/K/03, Government of Malaysia.

AUTHORS' CONTRIBUTIONS

All authors contributed equally to the completion in this study. Hazwani Mohd Yusof contributed to the idea, collected data, and contributed to manuscript writing. Sharaniza Ab-Rahim contributed to the idea, manuscript analysis, and review. Wan Zurinah Wan Ngah and Sheila Nathan contributed to the idea. A. Rahman A. Jamal contributed to the idea and obtained funding for this study. Musalmah Mazlan conceived

the idea, contributed to the application for funding, reviewed and edited the manuscript.

CONFLICTS OF INTEREST

The authors declare that there are no conflicts of interest.

REFERENCES

1. Bray F, Ferlay J, Soerjomataram I, Siegel RL, Torre LA, Jemal A, et al. Global cancer statistics 2018: GLOBOCAN estimates of incidence and mortality worldwide for 36 cancers in 185 countries. *CA Cancer J Clin* 2018;68:394-424.
2. Ferlay J, Soerjomataram I, Dikshit R, Eser S, Mathers C, Rebelo M, et al. Cancer incidence and mortality worldwide: Sources, methods and major patterns in GLOBOCAN 2012. *Int J Cancer* 2015;136:E359-86.
3. Compton CC, Greene FL. The staging of colorectal cancer: 2004 and beyond. *CA Cancer J Clin* 2004;54:295-308.
4. Provenzale D, Jasperson K, Ahnen DJ, Aslanian H, Bray T, Cannon JA, et al. Colorectal cancer screening, version 1.2015. *J Natl Compr Canc Netw* 2015;13:959-68.
5. Bretthauer M. Evidence for colorectal cancer screening. *Best Pract Res Clin Gastroenterol* 2010;24:417-25.
6. Society AC. Colorectal Cancer Facts and Figures 2017-2019. Atlanta: American Cancer Society; 2017.
7. Elia DH, El-Sibai M. Treatment strategies in colorectal cancer. In: Colorectal Cancer-Diagnosis, Screening and Management. United Kingdom: IntechOpen; 2017.
8. Villas-Boas SG, Roessner U, Hansen MA, Smedsgaard J, Nielsen J. *Metabolome Analysis: An Introduction*. New Jersey: John Wiley and Sons; 2007.
9. Nishiumi S, Kobayashi T, Ikeda A, Yoshie T, Kibi M, Izumi Y, et al. A novel serum metabolomics-based diagnostic approach for colorectal cancer. *PLoS One* 2012;7:e40459.
10. Qiu Y, Cai G, Su M, Chen T, Liu Y, Xu Y, et al. Urinary metabolomic study on colorectal cancer. *J Proteome Res* 2010;9:1627-34.
11. Brown DG, Rao S, Weir TL, O'Malia J, Bazan M, Brown RJ, et al. Metabolomics and metabolic pathway networks from human colorectal cancers, adjacent mucosa, and stool. *Cancer Metab* 2016;4:11.
12. Williams MD, Zhang X, Park JJ, Siems WF, Gang DR, Resar LM, et al. Characterizing metabolic changes in human colorectal cancer. *Anal Bioanal Chem* 2015;407:4581-95.
13. Tian Y, Xu T, Huang J, Zhang L, Xu S, Xiong B, et al. Tissue Metabonomic Phenotyping for Diagnosis and Prognosis of Human Colorectal Cancer. *Scientific Reports*; 2016. p. 6.
14. Wang H, Wang L, Zhang H, Deng P, Chen J, Zhou B, et al. ¹H NMR-based metabolic profiling of human rectal cancer tissue. *Mol Cancer* 2013;12:121.
15. Lin Y, Ma C, Liu C, Wang Z, Yang J, Liu X, et al. NMR-based fecal metabolomics fingerprinting as predictors of earlier diagnosis in patients with colorectal cancer. *Oncotarget* 2016;7:29454-64.
16. Yusof HM, Ab-Rahim S, Suddin LS, Saman MSA, Mazlan M. Metabolomics profiling on different stages of colorectal cancer: A systematic review. *Malays J Med Sci* 2018;25:16-34.
17. Cuperlovic-Culf M, Barnett DA, Culf AS, Chute I. Cell culture metabolomics: Applications and future directions. *Drug Discov Today* 2010;15:610-21.

18. Lauri I, Savorani F, Iaccarino N, Zizza P, Pavone LM, Novellino E, et al. Development of an optimized protocol for NMR metabolomics studies of human colon cancer cell lines and first insight from testing of the protocol using DNA G-quadruplex ligands as novel anti-cancer drugs. *Metabolites* 2016;6:E4.
19. Jiang W, Zhou L, Lin S, Li Y, Xiao S, Liu J, et al. Metabolic profiles of gastric cancer cell lines with different degrees of differentiation. *Int J Clin Exp Pathol* 2018;11:869-75.
20. Ser Z, Liu X, Tang NN, Locasale JW. Extraction parameters for metabolomics from cultured cells. *Anal Biochem* 2015;475:22-8.
21. Bannur Z, Teh LK, Hennesy T, Rosli WR, Mohamad N, Nasir A, et al. The differential metabolite profiles of acute lymphoblastic leukaemic patients treated with 6-mercaptopurine using untargeted metabolomics approach. *Clin Biochem* 2014;47:427-31.
22. Ehrig K, Kilinc MO, Chen NG, Stritzker J, Buckel L, Zhang Q, et al. Growth inhibition of different human colorectal cancer xenografts after a single intravenous injection of oncolytic vaccinia virus GLV-1h68. *J Transl Med* 2013;11:79.
23. Gatzidou E, Mantzourani M, Giaginis C, Giagini A, Patsouris E, Kouraklis G, et al. Augmenter of liver regeneration gene expression in human colon cancer cell lines and clinical tissue samples. *J BUON* 2015;20:84-91.
24. Orgeron ML, Stone KP, Wanders D, Cortez CC, Van NT, Gettys TW, et al. The impact of dietary methionine restriction on biomarkers of metabolic health. *Prog Mol Biol Transl Sci* 2014;121:351-76.
25. Borrego SL, Fahrman J, Datta R, Stringari C, Grapov D, Zeller M, et al. Metabolic changes associated with methionine stress sensitivity in MDA-MB-468 breast cancer cells. *Cancer Metab* 2016;4:9.
26. Cavuoto P, Fenech MF. A review of methionine dependency and the role of methionine restriction in cancer growth control and life-span extension. *Cancer Treat Rev* 2012;38:726-36.
27. Jeon H, Kim JH, Lee E, Jang YJ, Son JE, Kwon JY, et al. Methionine deprivation suppresses triple-negative breast cancer metastasis *in vitro* and *in vivo*. *Oncotarget* 2016;7:67223-34.
28. Giancaspero TA, Colella M, Brizio C, Difonzo G, Fiorino GM, Leone P, et al. Remaining challenges in cellular flavin cofactor homeostasis and flavoprotein biogenesis. *Front Chem* 2015;3:30.
29. Moat SJ, Ashfield-Watt PA, Powers HJ, Newcombe RG, McDowell IF. Effect of riboflavin status on the homocysteine-lowering effect of folate in relation to the MTHFR (C677T) genotype. *Clin Chem* 2003;49:295-302.
30. van den Donk M, Buijsse B, van den Berg SW, Ocké MC, Harryvan JL, Nagengast FM, et al. Dietary intake of folate and riboflavin, MTHFR C677T genotype, and colorectal adenoma risk: A dutch case-control study. *Cancer Epidemiol Biomarkers Prev* 2005;14:1562-6.
31. Nakano E, Mushtaq S, Heath PR, Lee ES, Bury JP, Riley SA, et al. Riboflavin depletion impairs cell proliferation in adult human duodenum: Identification of potential effectors. *Dig Dis Sci* 2011;56:1007-19.
32. Fadaka A, Ajiboye B, Ojo O, Adewale O, Olayide I, Emuwohochere R. Biology of glucose metabolism in cancer cells. *J Oncol Sci* 2017;3:45-51.
33. Rodríguez-Enríquez S, Juárez O, Rodríguez-Zavala JS, Moreno-Sánchez R. Multisite control of the crabtree effect in ascites hepatoma cells. *Eur J Biochem* 2001;268:2512-9.
34. Diaz-Ruiz R, Rigoulet M, Devin A. The warburg and crabtree effects: On the origin of cancer cell energy metabolism and of yeast glucose repression. *Biochim Biophys Acta* 2011;1807:568-76.
35. Vance JE, Vance DE. *Biochemistry of Lipids, Lipoproteins and Membranes*. Amsterdam: Elsevier; 2008.
36. Santos CR, Schulze A. Lipid metabolism in cancer. *FEBS J* 2012;279:2610-23.